EDGE ARTICLE

Check for updates

All publication charges for this article have been paid for by the Royal Society of Chemistry

A novel two-photon ratiometric fluorescent probe for imaging and sensing of BACE1 in different regions of AD mouse brain†

Lihong Ge, Zhichao Liu and Yang Tian [iD] *

β-Secretase (BACE1) is the vital enzyme in the pathogenic processes of Alzheimer's disease (AD). However, the development of a powerful tool with high selectivity and sensitivity for BACE1 determination *in vivo* is a challenge in understanding the pathogenesis of AD. In this work, a novel two-photon ratiometric fluorescent probe (AF633mCyd) was first developed for imaging and sensing of BACE1 in live cells and deep tissues, in which the fluorescence resonance energy transfer (FRET) system was designed and synthesized by a novel two-photon donor, merocyanine derivative (mCyd), connected with an acceptor, Alexa Fluor 633 (AF633), through a peptide substrate (EVNL-DAEFRHDSGYK) with a length of less than 10 nm. The emission spectrum of mCyd possessed sufficient overlap with the absorption spectrum of AF633, resulting in the high sensitivity of the developed AF633mCyd probe. The peptide substrate which can be specifically cleaved by BACE1 was inserted between the donor and acceptor, leading to the high selectivity of the present fluorescent probe. The fluorescence emission peaks of the AF633mCyd probe were observed at 578 nm and 651 nm and the emission ratio demonstrated good linearity with the concentration of BACE1 varying from 0.1 to 40.0 nM with a detection limit down to 65.3 ± 0.1 pM. Considering the advantages of high selectivity and sensitivity, as well as long-term stability and good biocompatibility, the developed probe was successfully applied in imaging and sensing of BACE1 in different regions of AD mouse brain tissue with a depth greater than 300 μm. Using this powerful tool, it was clear that the level of BACE1 was different in various brain regions of AD mouse such as S1BF, CPu, LD, and CA1. The up-regulation of BACE1 was observed especially in the regions S1BF and CA1 in AD mouse brain. Moreover, BACE1 was also found to be closely related to AD pathogenesis caused by oxidative stress.

Introduction

β-Secretase (BACE1) is an aspartic protease that plays a crucial role in the pathogenesis of Alzheimer's disease (AD).[1,2] BACE1 promotes the production of a C-terminal fragment containing 99 amino acids (CTFβ) by mediating cleavage of the amyloid precursor protein (APP) at the β site. CTFβ undergoes further processing by γ-secretase to release amyloid β (Aβ).[3–5] Accumulation of Aβ fragments in brain tissue causes the formation of aggregated species and insoluble fibrils mainly responsible for AD.[6,7] Collectively, BACE1 is the key enzyme in amyloidogenic processing of APP for Aβ formation. In addition, BACE1 has a significant connection with oxidative stress in the brain tissue of patients with AD.[8] However, the processes are unclear at the present stage. Developing a reliable probe for the determination of BACE1 with high selectivity and sensitivity for understanding the pathogenic processes of AD and evaluating the relationship between oxidative stress and BACE1 is a bottleneck.

Fluorescence sensors have attracted intense attention, since they provide high sensitivity with non-invasive features.[9–21] Up to now, a number of elegant fluorescent probes have been developed for imaging of BACE1.[22–26] Unfortunately, all of them are one-photon fluorescent probes using excitation wavelengths from the UV to visible range. In contrast, two-photon fluorescent probes utilizing two near-infrared photons of lower energy can offer deeper penetration (>300 μm) and lower background fluorescence.[27,28] Moreover, combined with the method with built-in correction, a two-photon ratiometric fluorescent probe possesses high reliability since it is independent of probe concentration, light source drift and complex environmental effects.[29,30] Our group is focusing on the development of novel probes for sensing of biological species in living cells, tissues,

Department of Chemistry, School of Chemistry and Molecular Engineering, East China Normal University, Dongchuan Road 500, Shanghai 200241, China. E-mail: ytian@chem.ecnu.edu.cn

† Electronic supplementary information (ESI) available: NMR spectra and HR-MS spectra; effects of pH on the responses of mCyd, AF633 and AF633mCyd probes; two-photon action spectra of mCyd and AF633; sensing mechanism; selectivity and competition tests; FACS and MTT tests of the AF633mCyd probe; MTT test of $O_2^{\cdot-}$ toward live cells; picture of mouse brain slices; and western blot images of BACE1 in different regions of mouse brain. See DOI: 10.1039/c9sc05256a

and *in vivo*.[31–33] However, to the best of our knowledge, the two-photon ratiometric fluorescent probe for the determination of BACE1 has never been reported.
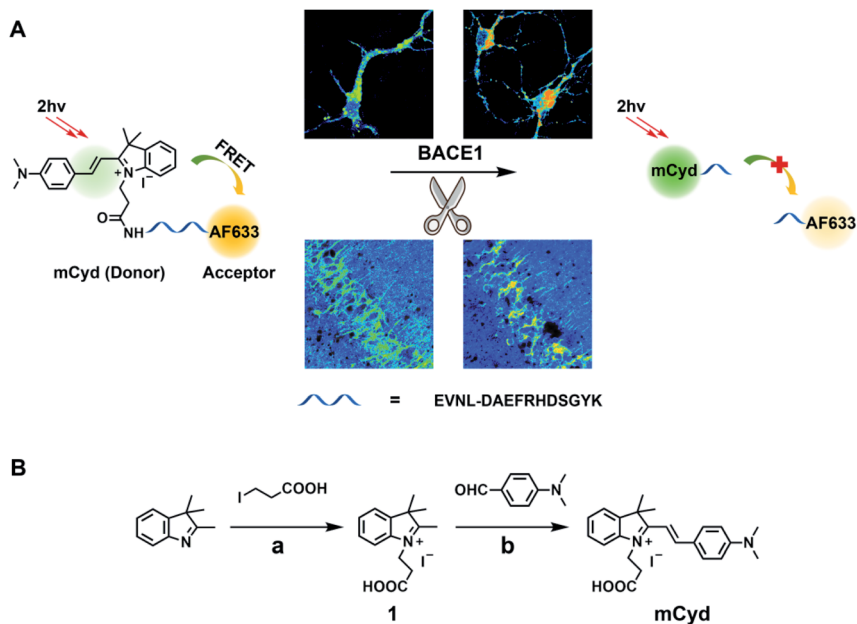
Herein, a novel two-photon ratiometric fluorescent probe (named AF633mCyd) was created for bioimaging and sensing of BACE1, in which a fluorescence resonance energy transfer (FRET) system containing an acceptor and a donor which were connected by the specific recognition element with a chain length less than 10 nm was constructed, as shown in Scheme 1A. First of all, a far visible dye, Alexa Fluor 633 (AF633), was optimized as the FRET acceptor. The fluorescent emission peak of AF633 was observed at 651 nm. Then, a novel two-photon dye, merocyanine derivative (mCyd), was designed and synthesized as the FRET donor, which fulfils three requirements: (1) the emission of mCyd possesses sufficient spectral overlap with AF633 absorption; (2) AF633 emits weakly at the optimal two-photon excitation wavelength of mCyd; (3) the dye maintains a stable fluorescence response at pH values ranging from 4.0 to 10.0 to meet the physiological acidic environment of the endosome in which BACE1 gains activity.[34] The fluorescence emission peak of the synthesized mCyd was obtained at 578 nm. Furthermore, for specific recognition of BACE1, the peptide substrate (EVNL-DAEFRHDSGYK, length < 10 nm) was inserted between the donor and acceptor, because it can be cleaved by BACE1 at the β site with high selectivity, leading to the separation of the donor and acceptor in the present FRET system. The first eight amino acids EVNL-DAEF of the peptide are important for BACE1 recognition and contain the enzyme cleavage site between leucine and aspartic acid (β site), which have been shown to be efficiently cleaved by BACE1 in the work by Franz and co-workers.[26,35] The remaining residues, RHDSGYK, serve to prevent the bulky AF633 dye from interfering in BACE1 hydrolysis. As a result, the developed AF633mCyd probe showed good selectivity for the determination of BACE1 against pepsin, thrombin, trypsin, α/γ-secretase, and so on. Two fluorescence emission peaks for the AF633mCyd probe were clearly observed at 578 nm and 651 nm, ascribed to the designed mCyd and AF633 dyes, respectively. With the probe being cleaved by BACE1, the fluorescence intensity at 578 nm was increased accompanied by the decrease of that at 651 nm as the energy transfer from mCyd to AF633 was inhibited. The fluorescence emission ratio of AF633mCyd displayed good linearity with the concentration of BACE1 from 0.1 to 40.0 nM with the detection limit (LOD) down to 65.3 ± 0.1 pM. Finally, considering the advantages of high selectivity, sensitivity and good biocompatibility, the developed two-photon probe, AF633mCyd, was applied for imaging and sensing of BACE1 in different regions of AD mouse brain tissue. From two-photon microscope images of BACE1 in the brain, it was found that the level of BACE1 was different in different regions of AD mouse brain such as primary somatosensory cortex (S1BF), caudate putamen (CPu), laterodorsal thalamic nucleus (LD), and field CA1 of the hippocampus (CA1). The up-regulation of BACE1 was observed especially in the regions of S1BF and CA1 in AD mouse brain. We also found that BACE1 exhibited a close relationship to AD pathogenesis caused by oxidative stress.

Results and discussion

Design and characterization of AF633mCyd

As a starting point, a far visible emission dye, AF633, was chosen as the FRET acceptor which possesses high resistance to acid interference,[36] to meet the physiological acidic environment of

Scheme 1 (A) Illustration for the working principle of the designed two-photon ratiometric fluorescent probe AF633mCyd for the determination of BACE1 in neurons and mouse brain tissue slice. (B) Synthesis steps for mCyd. Reaction conditions: (a) MeCN, 78 °C, 48 h, 82%; (b) CH₃COONa, EtOH, 75 °C, 6 h, 79%.

the endosome in which BACE1 gains activity.[34] The fluorescence emission peak of AF633 was clearly observed at 651 nm, as given in Fig. 1A. Then, a novel two-photon mCyd dye was designed and synthesized as the FRET donor. The synthesis steps of mCyd are illustrated in Scheme 1B. The synthesized processes for the mCyd dye were tracked and characterized by NMR and HR-MS (Fig. S1–S6, ESI†). As demonstrated in Fig. 1A, the fluorescence emission peak for mCyd was observed at 578 nm, which exhibits sufficient spectral overlap with the absorption of the acceptor AF633. The mCyd molecule also demonstrated good resistance to acid interference, suitable for BACE1 determination in the endosome (Fig. S7A, ESI†). Meanwhile, the two-photon action spectra of mCyd and AF633 dyes were measured (Fig. S8, ESI†).[37–41] mCyd showed the maximum two-photon action cross sections value (σ', 18.8 ± 1.9 GM) and AF633 demonstrated a small σ' value (3.9 ± 0.5 GM) when excited at 820 nm wavelength. Thus, the optimal excitation wavelength of AF633mCyd was 820 nm.

In the recognition unit of AF633mCyd, the peptide substrate (EVNL-DAEFRHDSGYK) with a length of less than 10 nm was selected to connect the donor and acceptor, which can be cleaved by BACE1 at the β site with high selectivity.[26,35] The stability of AF633mCyd under different pH values was examined. No obvious changes for F_{green}/F_{red} (<3.6%) were obtained, indicating the stable structure of this developed probe and its qualification for use in live systems (Fig. S7B, ESI†). The photostability of AF633mCyd was also examined. As shown in Fig. 1B, no significant changes of AF633mCyd in the emission

area ratio F_{green}/F_{red} (F_{green}: 560–620 nm, F_{red}: 640–700 nm) were observed in the absence (<1.5%) or presence (<4.3%) of BACE1 upon being exposed to 820 nm excitation for ~3 h, indicating long-term photostability of the developed fluorescent probe.

Next, the sensing mechanism of the AF633mCyd probe was verified by HR-MS. In Fig. S9 (ESI†), the peaks at 1010.6811 and 758.2645 correspond to the +H and +2H ions of AF633mCyd. In Fig. S10 (ESI†), the peak at 818.4430 corresponds to the N-terminus fragment of the AF633mCyd probe cleaved at the β site. The peaks at 1115.8012 and 744.2013 correspond to the +H and +2H ions of the C-terminus fragment of the AF633mCyd probe cleaved at the β site. Furthermore, the FRET mechanism for the determination of BACE1 using the AF633mCyd probe was studied. From Fig. 1C, the two-photon fluorescence spectrum of the AF633mCyd probe displayed two emission peaks at 578 nm and 651 nm, ascribed to the donor mCyd and acceptor AF633 dyes, respectively. The intensity of the donor significantly went up and that of the acceptor went down, as the AF633mCyd probe was cleaved by BACE1 leading to the separation of the donor and acceptor in this system. The results suggest that there was efficient energy transfer between mCyd and AF633. Moreover, the fluorescence lifetime of the donor mCyd (τ_D) was measured, as given in Fig. 1D. The initial value of τ_D was 1.3 ns, but it was decreased to 0.6 ns after being connected with AF633 to form the AF633mCyd probe. Then, τ_D turned back to 0.9 ns after the addition of BACE1 to the probe. The observation demonstrates an obvious energy transfer from mCyd to AF633, since energy transfer from the donor to acceptor would result in a decrease of the lifetime of the donor.[42]
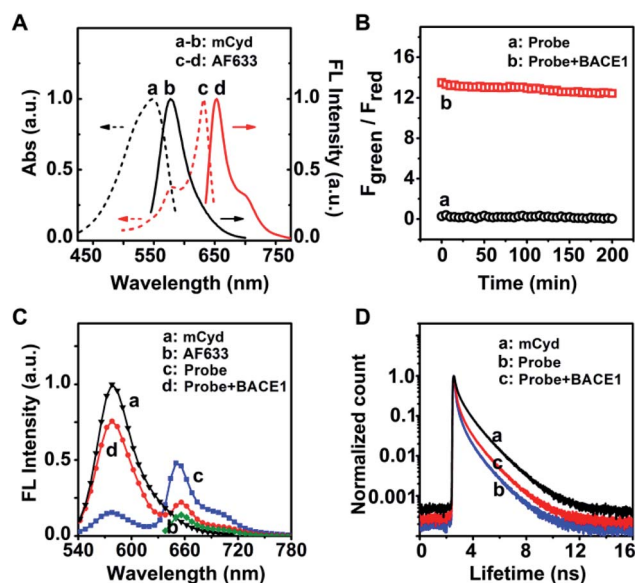

Fig. 1 (A) UV-vis absorption spectra and one-photon fluorescence spectra of (a and b) mCyd and (c and d) AF633. (B) Photostability test of the AF633mCyd probe before (a) and after (b) addition of BACE1. (C) Two-photon fluorescence spectra of (a) mCyd, (b) AF633, (c) AF633mCyd probe, and (d) AF633mCyd probe with the addition of BACE1, excited at 820 nm. (D) Fluorescence lifetime decay curves of (a) the donor mCyd, the donor mCyd part in this probe (b) without and (c) with the addition of BACE1. Spectra and lifetime were measured in 10 mM PBS containing 0.05% DMSO, pH = 4.5.

Two-photon fluorescence responses of the AF633mCyd probe toward BACE1 *in vitro*

Next, the titration of the developed probe AF633mCyd toward BACE1 was carried out. Fig. 2A illustrates the two-photon fluorescence spectra of 5.0 μM AF633mCyd with continuous addition of BACE1 to fresh cell lysates (containing 0.05% DMSO, pH was adjusted to 4.5 to maintain activity for BACE1) upon 820 nm excitation. The F_{green} (560–620 nm) increased dramatically and F_{red} (640–700 nm) gradually decreased with increasing concentration of BACE1. As plotted in Fig. 2B, F_{green}/F_{red} of the AF633mCyd probe shows a good linear correlation ($R^2 = 0.9971$) with the concentration of BACE1 varying from 0.1 to 40.0 nM. The regression equation was estimated as $F_{green}/F_{red} = 0.30 + 0.36$[BACE1] nM. The detection limit (LOD) was estimated to be down to 65.3 ± 0.1 pM ($3N/S$, N = the population standard deviation of blank sample, $n = 20$, S = the slope of calibration curve). The developed probe demonstrated a broader linear range and higher sensitivity for the determination of BACE1, compared with previously reported methods.[22–26]

The selectivity of the AF633mCyd probe toward BACE1 was also investigated in detail. As shown in Fig. 2C, the fluorescence responses for a series of potential interferences such as trypsin, cathepsin D (CD), α/γ-secretase, bromelain, thrombin, immunoglobulin G (IgG) and pepsin (500.0 nM for each) were checked. Negligible fluorescence changes were obtained (<4.6%). Furthermore, the selectivity of AF633mCyd for the
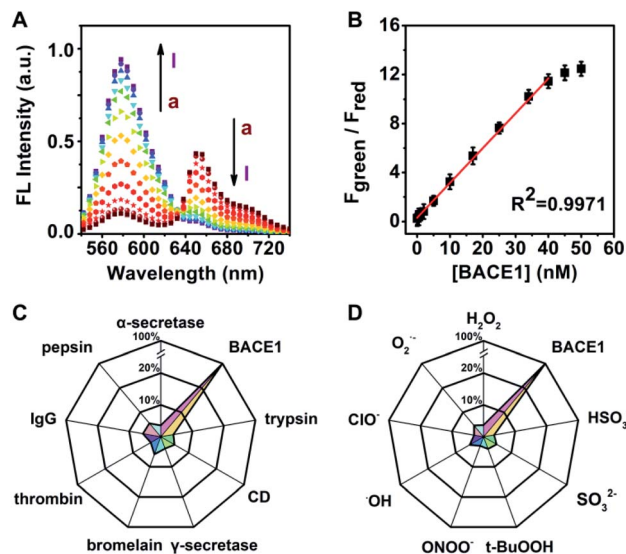
Fig. 2 (A) Two-photon fluorescence spectra of 5.0 μM AF633mCyd probe with the addition of BACE1 at different concentrations ((a) 0.0 nM, (b) 0.1 nM, (c) 0.5 nM, (d) 2.0 nM, (e) 5.0 nM, (f) 10.0 nM, (g) 17.0 nM, (h) 25.0 nM, (i) 34.0 nM, (j) 40.0 nM, (k) 45.0 nM, and (l) 50.0 nM), excited at 820 nm. (B) The plot between F_{green}/F_{red} (F_{green}: 560−620 nm, F_{red}: 640−700 nm) of the AF633mCyd probe and BACE1 concentrations (error bars, $n = 6$, SD). (C) Selectivity test of 5.0 μM AF633mCyd toward proteins such as trypsin, CD, α/γ-secretase, bromelain, thrombin, IgG and pepsin (500.0 nM each). (D) Selectivity test of 5.0 μM AF633mCyd toward ROS and other anions (1.0 mM each). The titration curve and selectivity were obtained in fresh cell lysates containing 0.05% DMSO, pH = 4.5.

determination of BACE1 was also studied, against reactive oxygen species (ROS), metal ions (1.0 mM for each), and so on, as shown in Fig. 2D and S11 (ESI†). No obvious changes for F_{green}/F_{red} (<2.8%) were obtained, indicating high selectivity of this developed probe for BACE1 detection. In the competition test (Fig. S11, ESI†), the addition of interfering species (trypsin, CD, α/γ-secretase, bromelain, thrombin, IgG, pepsin, ROS, metal ions, and other anions) induced negligible impacts (<3.1%) on BACE1 determination. Taken together, all the results demonstrated that the developed AF633mCyd probe recognized BACE1 with high selectivity, which should be ascribed to the selective peptide substrate toward BACE1.

Multicolor imaging of BACE1 in neurons

As demonstrated above, the developed probe AF633mCyd showed high selectivity, sensitivity, and long-term photo-stability for BACE1 detection, which were very beneficial for imaging of BACE1 in a living system. Before AF633mCyd was utilized to monitor endogenous BACE1 in living cells and tissues, biocompatibility and cytotoxicity of this probe were evaluated. In the flow cytometry (FACS) experiment, as shown in Fig. S12 and S13 (ESI†), the percentages of live cells (SYSH-5Y cells and neurons) were higher than 97% and those of dead cells were lower than 0.7% after the cells were incubated with a dose of 80.0 μM AF633mCyd probe, which was greater than that employed in bioimaging (5.0 μM) in live cells and tissues.

Meanwhile, in 3-(4,5-dimethylthiazol-2yl)-2,5-diphenylte-trazolium bromide (MTT) assay (Fig. S14†), the cells maintained high viability (>94%) using a dose of 80.0 μM AF633mCyd. These results demonstrated that the developed probe AF633mCyd exhibited good biocompatibility and low cytotoxicity.

Next, for imaging and sensing of endogenous BACE1 in live neurons, 5.0 μM AF633mCyd probe was incubated with neurons for 20 min. From Fig. 3A, we can see that the probe successfully entered into the neurons as shown in the overlay channel, and the value of F_{green}/F_{red} was calculated to be 3.8 ± 0.2. With increasing concentration of Axon 1125, a critical inhibitor of BACE1,[43] from 5.0 to 100.0 nM, the pseudocolor of the F_{green}/F_{red} channel turned from green to blue (Fig. 3B) and the value of F_{green}/F_{red} was reduced from 3.3 ± 0.2 to 2.0 ± 0.1 (Fig. 3C). These results revealed that the ratio of the F_{green}/F_{red} channel in neurons was decreased when BACE1 was suppressed, demon-strating that the developed AF633mCyd probe was quite quali-fied for endogenous BACE1 detection as expected.

The fluctuations of BACE1 in neurons were then studied under oxidative stress. Neurons were stimulated by superoxide ($O_2^{\bullet-}$), since $O_2^{\bullet-}$ is the primary ROS and considered to be an influential pro-oxidant model that induces oxidative stress.[44] First, the viabilities of neurons stimulated with different concentrations of $O_2^{\bullet-}$ were tested by MTT assay as shown in
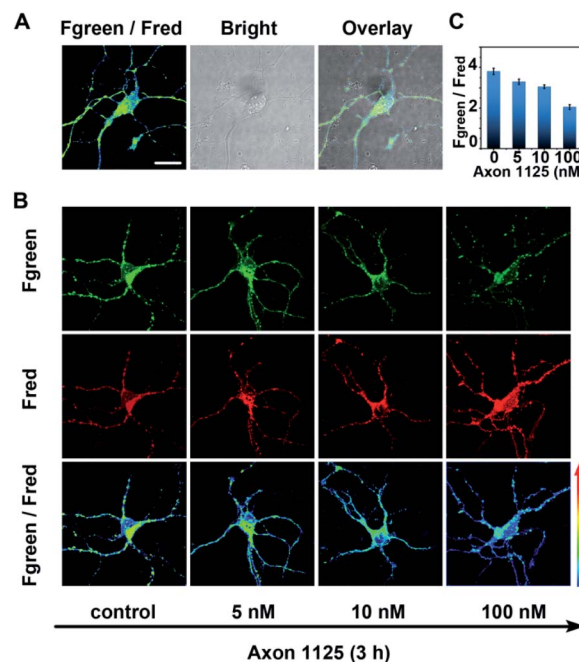

Fig. 3 (A) Two-photon microscope imaging of BACE1 in neurons. The green and red channels: fluorescence emission collected from 560−620 nm (F_{green}) and 640−700 nm (F_{red}), respectively. Overlay images were obtained from the F_{green}/F_{red} channel and bright image. (B) Two-photon microscope imaging of BACE1 in neurons treated with 0.0−100.0 nM Axon 1125 for 3 h. (C) The changes of F_{green}/F_{red} in neurons with increasing concentrations of Axon 1125. More than 50 neurons were evaluated for the statistical analyses (error bars, $n = 50$, SD). Scale bar = 25 μm.

Fig. S15 (ESI†). Neurons were treated with 0.0–50.0 μM $O_2^{\cdot-}$ for 2–12 h. We found that the viability of neurons gradually decreased with increasing concentration of $O_2^{\cdot-}$ and prolonging stimulation time. The viability of cells was maintained at ~76% using a dose of 20.0 μM $O_2^{\cdot-}$ for 12 h, but it was decreased to ~55% with a dose of 50.0 μM $O_2^{\cdot-}$ for 12 h. Thus, neurons were treated with 0.0–20.0 μM $O_2^{\cdot-}$ for 12 h or with 20.0 μM $O_2^{\cdot-}$ for 0–12 h to study the relationship between oxidative stress and BACE1 in the following experiments.

As shown in Fig. 4A and C, with the enhancement of the $O_2^{\cdot-}$ dose (0.0 to 20.0 μM), F_{green} went up markedly while F_{red} went down, the pseudocolour of the F_{green}/F_{red} channel changed from green to red, and the value of F_{green}/F_{red} increased from 3.7 ± 0.5 to 9.1 ± 0.3. These results explicitly indicated that BACE1 increased in neurons with increasing concentration of $O_2^{\cdot-}$. BACE1 in neurons after treatment with $O_2^{\cdot-}$ was further analyzed using western blot images. As shown in Fig. 4B and C, the increased BACE1 contents exhibited good agreement with those obtained from two-photon microscope imaging using the present AF633mCyd (BACE1/β-actin increased from 1.0 ± 0.1 to 2.2 ± 0.2). Meanwhile, the western blot images of CTFβ, the C-terminal fragment of APP after cleavage by BACE1, in neurons treated with $O_2^{\cdot-}$ were also obtained, since the CTFβ content changes could reflect the changes of BACE1 in neurons. As

shown in Fig. 4B and C, CTFβ was elevated obviously (CTFβ/β-actin increased from 1.0 ± 0.2 to 2.9 ± 0.2), confirming that BACE1 increased in neurons with the intensification of oxidative stress. On the other hand, in Fig. 4D and F, with prolonging stimulation time by 20.0 μM $O_2^{\cdot-}$ (0 to 12 h), the two-photon microscope imaging of the present AF633mCyd probe demonstrated that BACE1 was increased in neurons in a time-dependent manner. In Fig. 4E and F, the western blot images of BACE1 and CTFβ also displayed the same results as those obtained from confocal microscope images. Accordingly, the experimental results suggested that the level of BACE1 showed a close relationship with oxidative stress.

Imaging and sensing of BACE1 in different regions of AD brain tissues

Next, three dimensional (3D) one- and two-photon microscope images of the hippocampus region in AD mouse brain tissue labelled with the as-synthesized AF633mCyd probe were obtained. As shown in Fig. 5A and B, the two-photon microscope image offered deeper penetration (>300 μm) compared with the one-photon microscope image, which was in accordance with previous reports.[27,28] The AF633mCyd probe (5.0 μM) was subsequently used for evaluating the levels of BACE1 in AD (APP/PS1) and normal (C57BL/6) mouse brain tissues. Fig. 5C

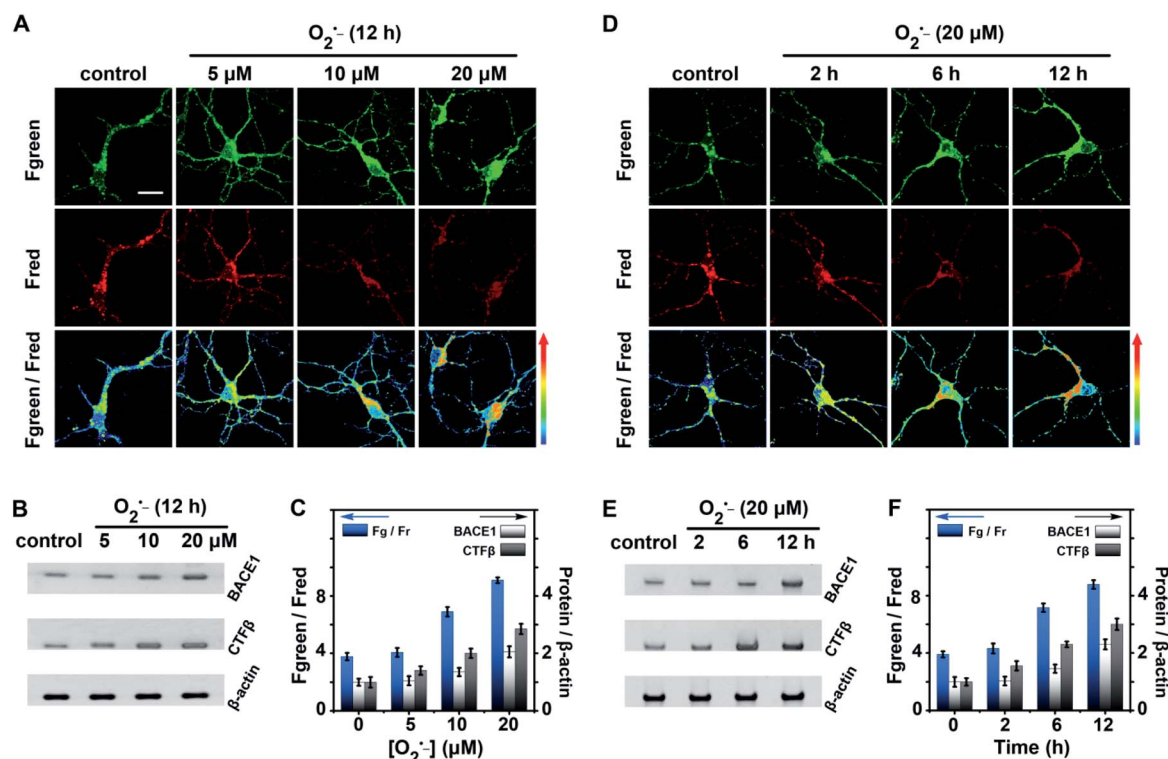**Fig. 4** (A) Two-photon microscope imaging of BACE1 in neurons treated with 0.0–20.0 μM $O_2^{\cdot-}$ for 12 h. (B) Western blot images of proteins (BACE1, CTFβ, and β-actin) obtained from neurons which were treated as (A). (C) F_{green}/F_{red} changes in neurons from (A) (left Y-axis); ratios of band density changes in (B) (right Y-axis). (D) Two-photon microscope imaging of BACE1 in neurons treated with 20.0 μM $O_2^{\cdot-}$ for 0–12 h. (E) Western blot images of proteins obtained from neurons which were treated as (D). (F) F_{green}/F_{red} changes in neurons from (D) (left Y-axis); ratios of band density changes in (E) (right Y-axis). The band densities were calculated using NIH ImageJ software. More than 50 neurons were evaluated for the statistical analyses (error bars, $n = 50$, SD). More than 20 parallel tests were carried out in (B) and (E). Proteins were visualized with BACE1, CTFβ, and β-actin specific antibodies, respectively. Scale bar = 25 μm.
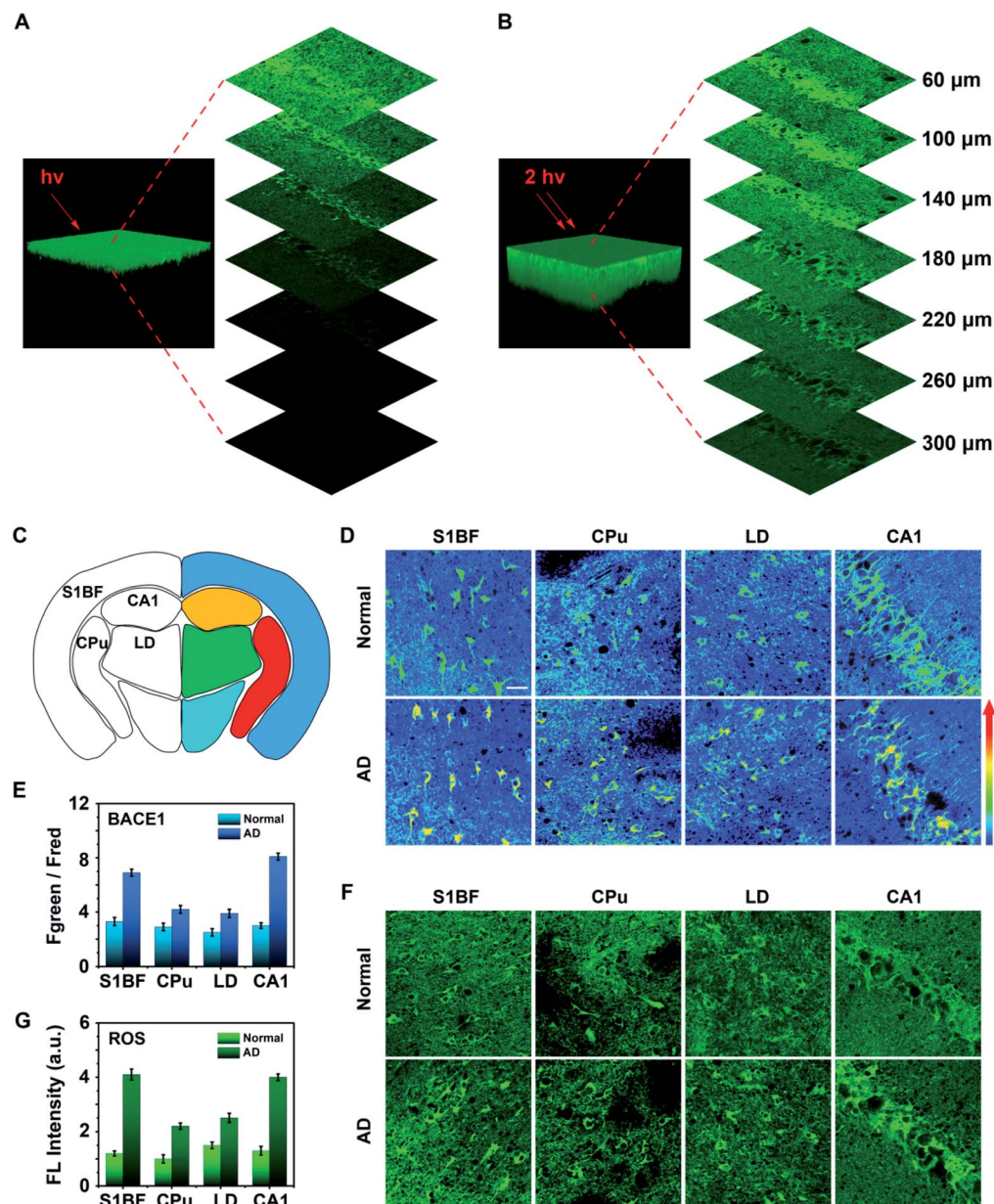
Fig. 5 Three dimensional (A) one-photon or (B) two-photon microscope images of the hippocampus region in AD mouse brain labelled with the AF633mCyd probe, excited at 552 nm and 820 nm, respectively. (C) Illustration for multiple regions of mouse brain slices (dark blue: cortex; red: striatum; green: thalamus; yellow: hippocampus). (D) Two-photon microscope images (overlay, F_{green}/F_{red}) of BACE1 using the AF633mCyd probe in S1BF, CPu, LD, and CA1 regions of AD and normal mouse brain slices. (E) F_{green}/F_{red} changes for BACE1 in S1BF, CPu, LD and CA1 regions in AD mouse brain slices compared with those in normal mouse brain. (F) Confocal microscope images of ROS using ROS commercial probe (DCFH-DA, ex/em = 480/525 nm, purchased from Yeasen Biotech Co. Ltd., China) in S1BF, CPu, LD, and CA1 regions of AD and normal mouse brain slices. Fluorescence emission collected from 500–560 nm, excited at 488 nm. (G) Fluorescence intensity changes for ROS in S1BF, CPu, LD, and CA1 regions of AD mouse brain slices compared with those of normal mouse brain. More than 20 mice were measured for the statistical analyses (error bars, $n = 20$, SD). Scale bar = 50 μm.

and S16 (ESI†) illustrates different regions of the mouse brain slice, such as primary somatosensory cortex (S1BF), caudate putamen (CPu), laterodorsal thalamic nucleus (LD), and field CA1 of hippocampus (CA1). From Fig. 5D, the pseudocolor of the F_{green}/F_{red} channel changed from green to orange in the regions S1BF, CPu, LD and CA1, demonstrating that BACE1 in these regions of AD mouse brain was higher than those in normal mouse brain. Interestingly, according to the statistical

analyses in Fig. 5E, the increases of F_{green}/F_{red} were remarkably pronounced in the S1BF and CA1 areas ($\sim$2.1-fold and $\sim$2.7-fold), compared with those in CPu and LD areas ($\sim$1.4-fold and $\sim$1.5-fold) in AD mouse brain. Then, BACE1 in different regions of AD and normal mouse brain tissues was analyzed using western blot images. As shown in Fig. S17 (ESI†), BACE1 contents obviously increased in S1BF and CA1 areas ($\sim$1.8-fold and $\sim$1.9-fold), compared with those in CPu and LD areas ($\sim$1.3-

fold and ∼1.2-fold) in AD mouse brain. These results demonstrated that the levels of BACE1 were nonuniform in different regions of AD mouse brain. It is well-known that the most significant clinical manifestation of AD is memory loss. Areas of the brain that are primarily involved in memory processing, such as the hippocampus and cortex, are likely to be first affected by disease pathology.[45–47] From the experimental results in Fig. 5D, E and S17 (ESI†) it can be seen that the levels of BACE1 in hippocampus and cortex areas were higher than those in other regions in AD mice, and therefore it can be considered that BACE1 levels were closely related to the pathogenesis of AD.

To further understand the interesting experimental phenomena, the ROS levels were detected in different areas of AD and normal mouse brains, because oxidative stress was likely to increase BACE1 gene promoter activity to cause BACE1 over transcription via several signaling pathways.[48] Fresh mouse brain tissue slices were stained with 10.0 μM DCFH-DA (a commercial ROS probe) to image. In Fig. 5F and G, the data showed that more enhancements of ROS were observed in the regions S1BF and CA1 (∼3.1-fold and ∼2.9-fold), compared with those obtained in CPu and LD areas (∼1.9-fold and ∼1.5-fold) in AD mouse brain. The results revealed that the intensification of oxidative stress was also pronounced in the hippocampus and cortex regions of AD mouse brain. Thus, it was found that both AD and oxidative stresses were closely associated with the level of BACE1.

Conclusions

In summary, a highly selective and sensitive two-photon ratiometric fluorescent probe, AF633mCyd, was rationally designed and developed for imaging and quantification of BACE1 in living cells and deep brain tissues, in which the FRET system was designed and synthesized using a novel two-photon donor mCyd, connected with an acceptor AF633, through a peptide substrate (EVNL-DAEFRHDSGYK, length < 10 nm). The spectra of mCyd and AF633 possessed sufficient overlap, resulting in enhancement in the sensitivity of the AF633mCyd probe. The peptide substrate which can be specifically cleaved by BACE1 was inserted between the donor and acceptor, leading to the high selectivity of the AF633mCyd probe. The developed fluorescent probe demonstrated high selectivity and sensitivity, as well as good biocompatibility and long-term stability. Thus, the AF633mCyd probe was successfully applied for imaging and sensing of BACE1 in live neurons and different regions of AD mouse brain tissue with a thickness of up to 300 μm. It was found that in the processes of oxidative stress-induced AD pathogenesis in mouse brain, the up-regulation of BACE1 was accomplished especially in the regions of S1BF and CA1. This study has successfully developed a reliable tool for live cell imaging and sensing of BACE1, which should be very useful for understanding the physiological and pathological processes of the brain.

Experimental section

Chemicals and reagents

2,3,3-Trimethylindolenine, 3-iodopropionic acid, 4-dimethylaminobenzaldehyde, acetonitrile (MeCN), ethanol (EtOH), diethyl ether, N,N-dimethylformamide (DMF), hydrogen peroxide (H_2O_2), tert-butyl hydroperoxide (t-BuOOH) and o-benzotriazole-N,N,N',N'-tetramethyl-uronium-hexafluorophosphate (HBTU) were purchased from J&K Chemical Co. Ltd. (Shanghai, China). Inorganic salts including CH_3COONa, CuCl, $Zn(NO_3)_2 \cdot 6H_2O$, $FeCl_2$, $CuCl_2$, $MgCl_2 \cdot 6H_2O$, $NiCl_2 \cdot 6H_2O$, $CdSO_4$, $CaCl_2$, $FeCl_3$, $AlCl_3$, $NaHSO_3$, Na_2SO_3, NaClO, NaCl, KCl, $NaHCO_3$, NaH_2PO_4, and $MgSO_4$ were obtained from Sinopharm Chemical Reagent Co. Ltd. (Shanghai, China). Peroxynitrite ($ONOO^-$) was derived from the reaction of H_2O_2 (25.0 μM) and $NaNO_2$ (25.0 μM). KO_2 was dissolved in anhydrous dimethyl sulfoxide (DMSO) to generate superoxide anions ($O_2^{\cdot-}$). Hydroxyl radical ($^\cdot OH$) was prepared by the Fenton reaction ($Fe^{2+}/H_2O_2 = 1:6$). The concentrations of $O_2^{\cdot-}$, $ONOO^-$ and H_2O_2 were determined by UV-vis absorption spectrometry.

Recombinant human BACE1 protein was purchased from Abcam Co. Ltd. (UK). AF633 NHS ester, D-glucose, neurobasal medium, B27, L-glutamine and papain were purchased from ThermoFisher Scientific Co. Ltd. (USA). Axon 1125 was obtained from Axon Medchem Co. Ltd. (Netherlands). Antibodies against rabbit polyclonal CTFβ (751–770), rabbit polyclonal BACE1 and mouse monoclonal β-actin were purchased from Sigma-Aldrich Co. Ltd. (USA). The ROS detection assay kit (DCFH-DA) was purchased from Yeasen Biotech Co. Ltd. (Shanghai, China). All analytical experiments were performed using ultrapure water (18.2 MΩ cm).

Instruments and apparatus

Nuclear magnetic resonance (NMR) spectra were recorded on a Bruker nuclear magnetic resonance spectrometer (500 MHz, Germany). The mass spectra (MS) were obtained using a Bruker ESI time-of-flight mass spectrometer (Germany) and a Thermo Scientific Q Exactive Benchtop Orbitrap mass spectrometer (USA). The UV-vis absorption spectra were recorded using a Hitachi UH-5300 spectrometer (Japan). The one-photon fluorescence spectra were obtained using a Hitachi F-4500 fluorescence spectrometer (Japan). The two-photon fluorescence spectra were obtained on a Leica TCS SP8 confocal laser scanning microscope (Germany) equipped with a Coherent two-photon laser (USA). The fluorescence lifetime decay curves were measured on a Becker & Hickl SyPhotime-64 time-correlated single photon counting (TCSPC) module (Germany). The fresh mouse brain tissue slices were obtained using a Leica VT3000 vibrating-blade microtome (Germany) with a thickness of about 300 μm.

Synthesis of mCyd

Compound 1 was synthesized in accordance with Step a in Scheme 1B. 2,3,3-Trimethylindolenine (5.0 mmol) and 3-iodopropionic acid (5.0 mmol) were dissolved in anhydrous MeCN (6.0 mL) and then stirred at 78 °C for 48 h under an argon atmosphere. Afterwards, the mixture was recrystallized from diethyl ether to collect compound 1 as a light pink solid (82% yield). ^1H NMR (500 MHz, DMSO): δ 8.00–7.98 (m, 1H), 7.85–7.83 (m, 1H), 7.64–7.61 (m, 2H), 4.65 (t, J = 15.0 Hz, 2H), 2.98 (t, J = 15.0 Hz, 2H), 2.86 (s, 3H), and 1.53 (s, 6H); ^{13}C NMR (125
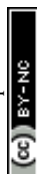
MHz, DMSO): δ 198.37, 171.98, 142.22, 141.29, 129.81, 129.38, 123.94, 116.02, 54.73, 44.00, 31.57, 22.34, and 14.84. HR-MS [M − I$^-$]$^+$: m/z calcd 232.1332, found 232.1333.

Next, mCyd was synthesized according to Step b in Scheme 1B. 4-dimethylaminobenzaldehyde (5.0 mmol) and CH_3COONa (5.0 mmol) were added to the solution of compound **1** (5.0 mmol) in anhydrous EtOH (8.0 mL) under an argon atmosphere and stirred at 75 °C for 6 h. The solvent was removed under reduced pressure after the reaction was completed. Then the crude product was further purified by silica gel chromatography with 12% MeOH in DCM as the eluent to obtain the desirable dark purple solid mCyd (79% yield). ^1H NMR (500 MHz, MeOD): δ 8.33 (d, J = 15.0 Hz, 1H), 8.00 (d, J = 10.0 Hz, 2H), 7.69–7.66 (m, 2H), 7.57–7.47 (m, 2H), 7.38 (d, J = 20.0 Hz, 1H), 6.90 (d, J = 10.0 Hz, 2H), 4.70 (t, J = 15.0 Hz, 2H), 3.21 (s, 6H), 2.75 (t, J = 15.0 Hz, 2H), and 1.82 (s, 6H); ^{13}C NMR (125 MHz, MeOD): δ 179.73, 155.25, 155.12, 142.65, 141.09, 128.75, 127.50, 122.63, 122.37, 113.20, 112.20, 104.40, 51.13, 43.17, 39.17, 35.65, and 26.20. HR-MS [M − I$^-$]$^+$: m/z calcd 363.2067, found 363.2067.

Design and synthesis of AF633mCyd

The sequence of AF633mCyd was (mCyd)-EVNL-DAEFRHDS-GYK (AF633)-NH$_2$. First of all, a far visible dye AF633 was optimized as the FRET acceptor. Then, a novel two-photon dye, merocyanine derivative (mCyd), was designed and synthesized as the FRET donor, which fulfils three requirements: (1) the emission of mCyd possesses sufficient spectral overlap with AF633 absorption; (2) AF633 emits weakly at the optimal two-photon excitation wavelength of mCyd; (3) the dye maintains a stable fluorescence response at pH values ranging from 4.0 to 10.0, to meet the physiological acidic environment of the endosome in which BACE1 gains activity.[39] Furthermore, for specific recognition of BACE1, the peptide substrate (EVNL-DAEFRHDSGYK, length < 10 nm) was inserted between the donor and acceptor, because it can be cleaved by BACE1 at the β site with high selectivity, leading to the separation of the donor and acceptor in the present FRET system.[26,35]

AF633mCyd was prepared by standard Fmoc solid-phase peptide synthesis. First, the precursor compounds Fmoc-Glu(mCyd)-OH and Fmoc-Lys(AF633)-OH were synthesized. The mCyd dye and AF633 dye were coupled to Glu and Lys respectively through amide bonds with HBTU in DMF for 20 min. Second, standard Fmoc-protected natural and non-natural amino acids were coupled in 20 min cycles with HBTU in DMF, to synthesize AF633mCyd. Third, the crude product was further purified by preparative chromatography to obtain AF633mCyd. The synthesis for AF633mCyd was supported by GL Biochem Co. Ltd. (Shanghai, China). HR-MS of the AF633mCyd probe [M − 2I$^-$ + 2H$^+$]$^{4+}$: m/z calcd 758.2646, found 758.2645. [M − 2I$^-$ + H$^+$]$^{3+}$: m/z calcd 1010.6837, found 1010.6811.

Determination of the two-photon action cross-section

First, the fluorescence quantum yield was calculated according to the following equation:[37]

$$\Phi_s = \Phi_r(A_r F_s n_s^2)/(A_s F_r n_r^2) \tag{1}$$

The subscripts s and r represent the sample and the reference molecule, respectively. Φ is the fluorescence quantum yield, A is the absorbance of the molecule that is controlled below 0.05, F means the integrated emission area, and n is the refractive index of the solvent. For the measurement of the fluorescence quantum yield of the mCyd dye (Φ_D) and AF633mCyd probe (Φ_P), rhodamine B (Φ = 0.71, MeOH) was chosen as the reference. The Φ_D and Φ_P were calculated to be 0.33 and 0.02, respectively. In addition, the value of the fluorescence quantum yield of the AF633 dye (Φ_A) was calculated to be 0.58 using sulforhodamine 101 (Φ = 0.95, EtOH) as the reference dye.[38]

Second, the two-photon cross-section (σ) was determined using the reference material contrast fluorescence measurement method, according to the following equation:[39]

$$\sigma_s = \sigma_r(F_s \Phi_r C_r n_r)/(F_r \Phi_s C_s n_s) \tag{2}$$

The subscripts s and r represent the sample and the reference molecule, respectively. F represents the measured two-photon fluorescence intensity, Φ is the fluorescence quantum yield, C is the concentration of the solution, and n is the refractive index of the solvent. For the measurement of the two-photon cross-section of mCyd and AF633 dyes, rhodamine B and tetraphenyl-porphine were selected as the references, respectively, which possessed a fluorescence maximum close to that of the sample in our study.[40]

Third, the two-photon action cross-section (σ') was obtained *via* the following equation:[41]

$$\sigma' = \Phi \times \sigma \tag{3}$$

Φ is the fluorescence quantum yield and σ is the two-photon cross section.

Culture and imaging of primary mouse cortical neurons

All animal experiments were performed according to the guidelines of the Care and Use of Laboratory Animals formulated by the Ministry of Science and Technology of China and were approved by the Animal Care and Use Committee of East China Normal University (approval no. m+ R20190304, Shanghai, China). Primary mouse cortical neurons were obtained *via* the reported experimental procedure.[35] First, the whole brain tissues of newborn C57BL/6 mice were taken out rapidly and immersed in Hanks' balanced salt solution (HBSS, free Mg^{2+} & Ca^{2+}) at 0 °C. Second, the tissues were preincubated with papain for 12 min at 37 °C and dissociated with a fire-polished glass pipette to obtain the neuron suspension. The neuron suspension was inoculated into a PDL-coated 35 mm culture dish at a density of 1 × 10^6 cells per dish. Finally, neurons were cultured in neurobasal medium supplemented with B27 and L-glutamine in a humidified incubator (5% CO$_2$/ 95% air, 37 °C). Neurons can be used for the assay after about 5 days of inoculation.

The two-photon confocal fluorescence images of adherent neurons were obtained on a Leica TCS SP8 confocal laser
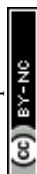
scanning microscope (Germany) equipped with a Coherent two-photon laser (USA), excited at 820 nm. Emissions were collected in green (560–620 nm) and red (640–700 nm) channels, respectively.

Preparation and imaging of mouse brain tissue slices

All animal experiments were performed according to the guidelines of the Care and Use of Laboratory Animals formulated by the Ministry of Science and Technology of China and were approved by the Animal Care and Use Committee of East China Normal University (approval no. m+ R20190304, Shanghai, China). The fresh mouse brain tissue slices were prepared according to the reported procedure.[32] Five-month-old normal mice and AD mice (APP/PS1) were purchased from the Laboratory Animal Center of the Chinese Academy of Science. First, the fresh mouse brain tissue slices were obtained using a Leica VT3000 vibrating-blade microtome (Germany) with a thickness of about 300 μm. This step was fully operated in ice-cold artificial cerebrospinal fluid (ACSF, NaCl 124.0 mM, KCl 3.0 mM, NaHCO$_3$ 26.0 mM, NaH$_2$PO$_4$ 1.24 mM, MgSO$_4$ 8.0 mM, CaCl$_2$ 0.1 mM and D-glucose 10.0 mM) under a 95% O$_2$ and 5% CO$_2$ atmosphere. Second, the slices were transferred to an incubation chamber filled with ACSF containing 20.0 μM AF633mCyd at 37 °C for 60 min, and the ACSF was aerated with 95% O$_2$ and 5% CO$_2$. The treated slices were then washed with ACSF at least three times for imaging. Finally, the stained slices were observed with a TCS-SP8 confocal laser-scanning microscope equipped with a multiple-photon laser, excited at 820 nm.

Conflicts of interest

There are no conflicts to declare.

Acknowledgements

Notes and references

1 I. Hussain, D. Powell, D. Howlett, D. Tew, T. Meek, C. Chapman, I. Gloger, K. Murphy, C. Southan, D. Ryan, T. Smith, D. Simmons, F. Walsh, C. Dingwall and G. Christie, *Mol. Cell. Neurosci.*, 1999, **14**, 419–427.

2 Y. Luo, B. Bolon, S. Kahn, B. Bennett, S. Khan, P. Denis, W. Fan, H. Kha, J. Zhang, Y. Gong, L. Martin, J. Louis, Q. Yan, W. Richards, M. Citron and R. Vassar, *Nat. Neurosci.*, 2001, **4**, 231–232.

3 R. Vassar, B. Bennett, S. Khan, S. Kahn, E. Mendiaz, P. Denis, D. Teplow, S. Ross, P. Amarante, R. Loeloff, Y. Luo, S. Fisher, J. Fuller, S. Edenson, J. Lile, M. Jarosinski, A. Biere, E. Curran, T. Burgess, J. Louis, F. Collins, J. Treanor, G. Rogers and M. Citron, *Science*, 1999, **286**, 735–741.

4 M. Wolfe, *Chem. Rev.*, 2009, **109**, 1599–1612.

5 A. Fernandez, K. Biette, G. Dolios, D. Seth, R. Wang and M. Wolfe, *Biochemistry*, 2016, **55**, 5675–5688.

6 S. Lesné, M. Koh, L. Kotilinek, R. Kayed, C. Glabe, A. Yang, M. Gallagher and K. Ashe, *Nature*, 2006, **440**, 352–357.

7 V. Villemagne, K. Pike, G. Chetelat, K. Ellis and R. Mulligan, *Ann. Neurol.*, 2011, **69**, 181–192.

8 E. Tamagno, M. Guglielmotto, D. Monteleone and M. Tabaton, *Neurotoxic. Res.*, 2012, **22**, 208–219.

9 P. Gao, W. Pan, N. Li and B. Tang, *Chem. Sci.*, 2019, **10**, 6035–6071.

10 X. Pan, Y. Zhao, T. Cheng, A. Zheng, A. Ge, L. Zang, K. Xu and B. Tang, *Chem. Sci.*, 2019, **10**, 8179–8186.

11 W. Zhang, J. Zhang, P. Li, J. Liu, D. Su and B. Tang, *Chem. Sci.*, 2019, **10**, 879–883.

12 T. Minami, T. Minamiki and S. Tokito, *Chem. Commun.*, 2015, **51**, 9491–9494.

13 T. Minami, N. Esipenko, A. Akdeniz, B. Zhang, L. Isaacs and P. Anzenbacher, *J. Am. Chem. Soc.*, 2013, **135**, 15238–15243.

14 Y. Sasaki, T. Minamiki, S. Tokito and T. Minami, *Chem. Commun.*, 2016, **52**, 7838–7841.

15 K. Kawai, Y. Osakada, M. Fujitsuka and T. Majima, *Chem. Commun.*, 2006, 3918–3920.

16 D. Liu, Y. Lv, M. Chen, D. Cheng, Z. Song, L. Yuan and X. Zhang, *J. Mater. Chem. B*, 2019, **7**, 3970–3975.

17 C. Jin, T. Fu, R. Wang, H. Liu, J. Zou, Z. Zhao, M. Ye, X. Zhang and W. Tan, *Chem. Sci.*, 2017, **8**, 7082–7086.

18 H. Liu, L. Chen, C. Xu, Z. Li, H. Zhang, X. Zhang and W. Tan, *Chem. Soc. Rev.*, 2018, **47**, 7140–7180.

19 J. Zhou, L. Li, W. Shi, X. Gao, X. Li and H. Ma, *Chem. Sci.*, 2015, **6**, 4884–4888.

20 X. He, L. Li, Y. Fang, W. Shi, X. Li and H. Ma, *Chem. Sci.*, 2017, **8**, 3479–3483.

21 Y. Fang, W. Shi, Y. Hu, X. Li and H. Ma, *Chem. Commun.*, 2018, **54**, 5454–5457.

22 X. Zuo, H. Dai, H. Zhang, J. Liu, S. Ma and X. Chen, *Analyst*, 2018, **143**, 4585–4591.

23 Y. Choi, Y. Cho, M. Kim, R. Grailhe and R. Song, *Anal. Chem.*, 2012, **84**, 8595–8601.

24 L. Liu, N. Xia and J. Yu, *Microchim. Acta*, 2016, **183**, 265–271.

25 J. Luo, A. Rasooly, L. Wang, K. Zeng, C. Shen, P. Qian, M. Yang and F. Qu, *Microchim. Acta*, 2016, **183**, 605–610.

26 D. Folk, J. Torosian, S. Hwang, D. McCafferty and K. Franz, *Angew. Chem., Int. Ed.*, 2012, **51**, 10795–10799.

27 F. Helmchen and W. Denk, *Nat. Methods*, 2005, **2**, 932–940.

28 E. Hoover and J. Squier, *Nat. Photonics*, 2013, **7**, 93–101.

29 M. Lee, J. Kim and J. Sessler, *Chem. Soc. Rev.*, 2015, **44**, 4185–4191.

30 X. Huang, J. Song, B. Yung, X. Huang, Y. Xiong and X. Chen, *Chem. Soc. Rev.*, 2018, **47**, 2873–2920.

31 L. Ge and Y. Tian, *Anal. Chem.*, 2019, **91**, 3294–3301.

32 W. Li, B. Fang, M. Jin and Y. Tian, *Anal. Chem.*, 2017, **89**, 2553–2560.

33 W. Wang, F. Zhao, M. Li, C. Zhang, Y. Shao and Y. Tian, *Angew. Chem., Int. Ed.*, 2019, **58**, 5256–5260.

34 S. Halima and L. Rajendran, *J. Alzheimer's Dis.*, 2011, **24**, 143–152.

35 D. Folk and K. Franz, *J. Am. Chem. Soc.*, 2010, **132**, 4994–4995.

36 D. Thompson, P. Wilson, M. Sims, D. Cullen, J. Holt, D. Parker and M. Smith, *Anal. Chem.*, 2006, **78**, 2738–2743.

37 J. Demas and G. Crosby, *J. Phys. Chem.*, 1971, **75**, 991–1024.

38 R. Velapoldi and H. Tonnesen, *J. Fluoresc.*, 2004, **14**, 465–472.

39 C. Xu and W. Webb, *J. Opt. Soc. Am. B*, 1996, **13**, 481–491.

40 N. Makarov, M. Drobizhev and A. Rebane, *Opt. Express*, 2008, **16**, 4029–4047.

41 L. Yuan, W. Lin, H. Chen, S. Zhu and L. He, *Angew. Chem., Int. Ed.*, 2013, **52**, 10018–10022.

42 W. Liu, F. Li, X. Chen, J. Hou, L. Yi and Y. Wu, *J. Am. Chem. Soc.*, 2014, **136**, 4468–4471.

43 S. Stachel, *J. Med. Chem.*, 2004, **47**, 6447–6450.

44 H. Sies, *Redox Biol.*, 2017, **11**, 613–619.

45 H. Fukumoto, B. Cheung, B. Hyman and M. Irizarry, *Arch. Neurol.*, 2002, **59**, 1381–1389.

46 X. Ye and Q. Cai, *Cell Rep.*, 2014, **6**, 24–31.

47 B. Zott, M. Busche, R. Sperling and A. Konnerth, *Annu. Rev. Neurosci.*, 2018, **41**, 277–297.

48 E. Tamagno, M. Guglielmotto, D. Monteleone and M. Tabaton, *Neurotoxic. Res.*, 2012, **22**, 208–219.